CMS TN/95-152
August 1995

Optical properties of lead tungstate ($PbWO_4$) crystal for LHC em-calorimetry

S. Baccaro (*), L. M. Barone, B. Borgia, F. Castelli (•), F. Cavallari, F. de Notaristefani, M. Diemoz, R. Faccini, A. Festinesi (*), E. Leonardi, E. Longo, M. Mattioli, M. Montecchi (*), G. Organtini, S. Paoletti, E. Valente

Dipartimento di Fisica, Università "La Sapienza", Roma
INFN - Sezione di Roma

(*) ENEA - INN, Casaccia, Roma

(•) Dipartimento di Chimica, Università "La Sapienza", Roma

Nota Interna n° 1066

Dipartimento di Fisica
Università "La Sapienza", Roma

INFN - Sezione di Roma

Abstract

This note reports the work carried out in order to determine the optical properties of $PbWO_4$ crystals. We performed transmission and reflectance measurements at normal incidence in the range 320-850 nm with polarised light and measurements of the separation angle γ between the ordinary and extraordinary rays with laser beam in the wavelength range mentioned above.

Stampato in proprio - P.le Aldo Moro, 2 - 00185 Roma

Finito di stampare il 28 agosto 1995

1 - Introduction

Crystals of $PbWO_4$ will be used in the electromagnetic calorimeter of the CMS experiment at LHC (CERN).

The behaviour of the electromagnetic wave generated in a crystal depends on the boundaries and on the refractive index (N) of the crystal itself. For an isotropic crystal, the refractive index N is a complex number depending only on the e.m. wavelength λ. At λ values where the crystal is transparent, the reflectance of the e.m. wave at the crystal-air interface depends mainly on the real part *n* of the refractive index N. On the other hand the attenuation of the e.m. wave, travelling through the crystal, depends on the imaginary part *k* of N, called extinction coefficient. The absorption coefficient α can be defined as

$$\alpha = 4\pi k / \lambda \ . \qquad (1)$$

Observation on the propagation of laser beam through $PbWO_4$ crystal leads us to consider $PbWO_4$ an optically anysotropic medium of uniaxial type. In this case, N also depends on the orientation of the electrical vector **E** of the e.m. wave and it can be represented by an index ellipsoid having two equal principal axes (revolution ellipsoid) [1]. The values of N along these two axes and along the third axis (the optical axis of the crystal) are respectively named ordinary and extraordinary index. This note describes a procedure for the determination of the crystal index ellipsoid. The proposed method entails the measurement of the transmission *T* and reflectance *R* at normal incidence with polarised light and the measurement of the separation angle γ between the ordinary and extraordinary rays at various wavelengths.

We investigated undoped and doped crystals: PWO-522 (1 cm length, undoped), PWO-N30 (23 cm length, undoped) and PWO-1024 (21.5 cm length, 30 ppm Nb^{5+} doped).

2 - Theory

2.1 - Propagation of a plane e.m. wave in uniaxial crystal

Let us consider an air-uniaxial crystal plane interface and a monochromatic e.m. plane wave travelling with the wave front parallel to the interface. In the general case the optical axis of the crystal has an angle β with the interface. Let be Γ the plane orthogonal to the interface containing the crystal optical axis. It is convenient to decompose the vector **E** into two components, one parallel $E_{//}$ and the other one $E_{\perp}$ orthogonal to the Γ plane. The wave corresponding to $E_{\perp}$ travels through the crystal according to the usual laws of an isotropic medium (ordinary ray), while the one corresponding to $E_{//}$ propagates with a velocity depending on β (extraordinary ray). Fig. 1 shows $E_{//}$ and the section of the index ellipsoid on the Γ plane. The orientation of the cross-section coordinate axes x, y was chosen so that y is parallel to the crystal optical axis. The component $E_{//}$ experiences the refractive index n_{mix} that is a mixing of ordinary and extraordinary refractive index given by

$$n_{mix} = n_{ord}\sqrt{\sin^2\beta + \frac{n_{ext}^2}{n_{ord}^2}\cos^2\beta} \tag{2}$$

Fig. 2 shows the section on the Γ plane of the elliptic wave front emitted from a point source located at the origin of the coordinate system of axes x, y. The elliptic wave front is described by the following equation

$$x^2 n_{ord}^2 + y^2 n_{ext}^2 = c^2 t^2 \tag{3}$$

or in terms of the emission angle ϕ, by the parametric form

$$\begin{cases} x = ct\cos\phi / n_{ord} \\ y = ct\sin\phi / n_{ext} \end{cases} \tag{4}$$

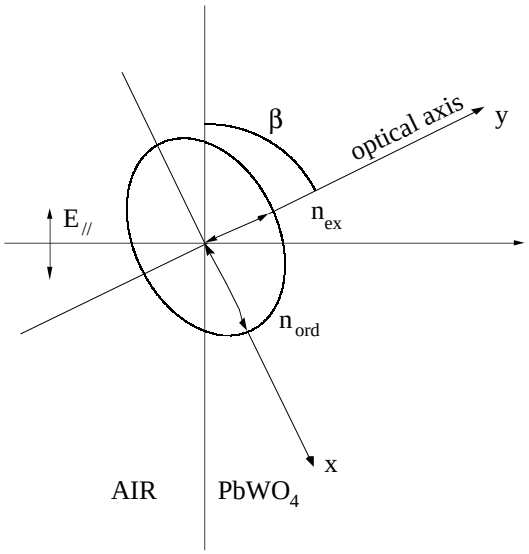

Fig. 1: Cross section of index ellipsoid on the Γ plane at the air-crystal interface. A plane wave falls orthogonally on the interface and the component $E_{//}$ of the **E** is depicted.

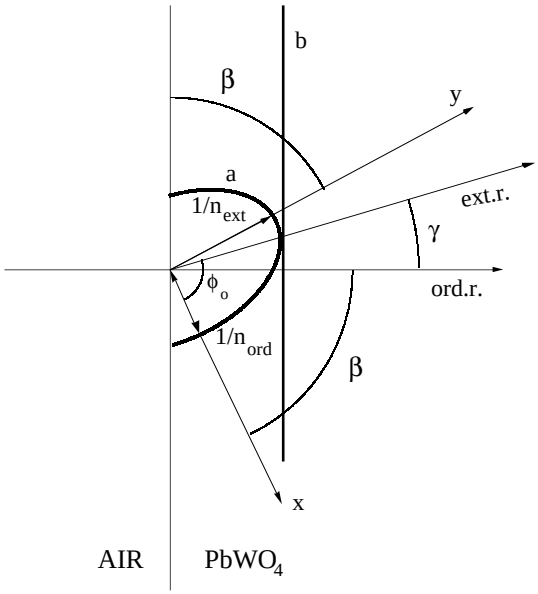

Fig. 2: Cross sections on the Γ plane a) of the ellipsoidal wave front emitted from a point source, located in x = 0 y = 0; and b) of the envelope representing the extraordinary wave.
β, ϕ_0 and γ are the angles between i) boundary-optical axis; ii) x axis-direction of extraordinary ray propagation; iii) ordinary ray-extraordinary ray respectively.

The wave front of the extraordinary ray is a plane parallel to the air-crystal interface. The straight line joining the point source and the point where the elliptic wave front is tangent to the extraordinary plane wave front, gives the direction of the extraordinary ray propagation. Let call ϕ_0 the angle between this direction and the x axis.
From the eq. (3) it follows

$$\frac{dy}{dx} = -\left(\frac{n_{ord}}{n_{ext}}\right)^2 \frac{x}{y} \tag{5}$$

that in terms of ϕ can be written as

$$\frac{dy}{dx} = -\frac{n_{ord}}{n_{ext}} \frac{1}{\tan\phi} \tag{6}$$

On the other hand for $\phi = \phi_0$ $\quad \frac{dy}{dx} = -\frac{1}{\tan\beta}$, so that

$$\tan\phi_0 = \frac{n_{ord}}{n_{ext}} \tan\beta \ . \tag{7}$$

The direction of the ordinary ray makes an angle β with the x axis so that finally the γ angle between the directions of the extraordinary and ordinary ray is given by

$$\gamma = \phi_0 - \beta = \text{atan}\left(\frac{n_{ord}}{n_{ext}}\tan\beta\right) - \beta \qquad (8)$$

Equation (8) relates γ with the ratio n_{ord}/n_{ext} and the β angle; the γ angle is equal to 0 either for an isotropic crystal ($n_{ext} = n_{ord}$) or when β = 0. The case β = 90° is trivial because in this case **E** cannot experience the extraordinary refractive index.
Both the orientation of the Γ plane and the γ angle can be easily determined by examining the propagation of a laser beam hitting orthogonally on a crystal surface if $0 < \beta < 90°$ and the crystal is long enough to allow the separation of the extraordinary from the ordinary beam. If the laser is linearly polarised and only one beam is visible in the crystal, **E** could be parallel or orthogonal to the Γ plane. After rotation by 45° of the laser or the sample, the two beams should be visible.

2.2 - Transmittance and reflectance spectrophotometric measurements at normal incidence with polarised light.

The transmittance and reflectance measurements on the air-crystal interface give further information and lead to the complete determination of the index ellipsoid.
When a plane wave falls on the air-crystal boundary, it splits into two waves: a transmitted one proceeding through the crystal and a reflected one propagating back into the air. At normal incidence, the transmittance and the reflectance of a plane wave are given by [1]

$$t = 1 - r \qquad r = \left|\frac{n-1}{n+1}\right|^2 \qquad (9)$$

where $n_{air} = 1$ and $k << n$ are assumed. Both *t* and *r* are independent from the direction of wave propagation. In the case of isotropic crystals at normal incidence, *t* and *r* do not depend on the light polarisation. On the contrary, in the case of uniaxial crystals, the light experiences the ordinary index or the mixed index of equation (2) if its polarisation is respectively orthogonal or parallel to the Γ plane. The measurements performed with these two polarisations give then independent information on optical properties of the crystal.

The $PbWO_4$ crystals are hexaedron and the measurements of the overall transmittance *T* and reflectance *R* involve not only the entrance air-crystal interface, but also the opposite one (Fig. 3). The reflectance measurement is performed at the incidence angle of about 7° (Fig. 3b). At this incidence angle, for an isotropic sample, the instrument sensitivity does not distinguish the reflectance of *p* polarised light from the s polarisation, therefore the measured reflectance can be treated like at normal incidence.

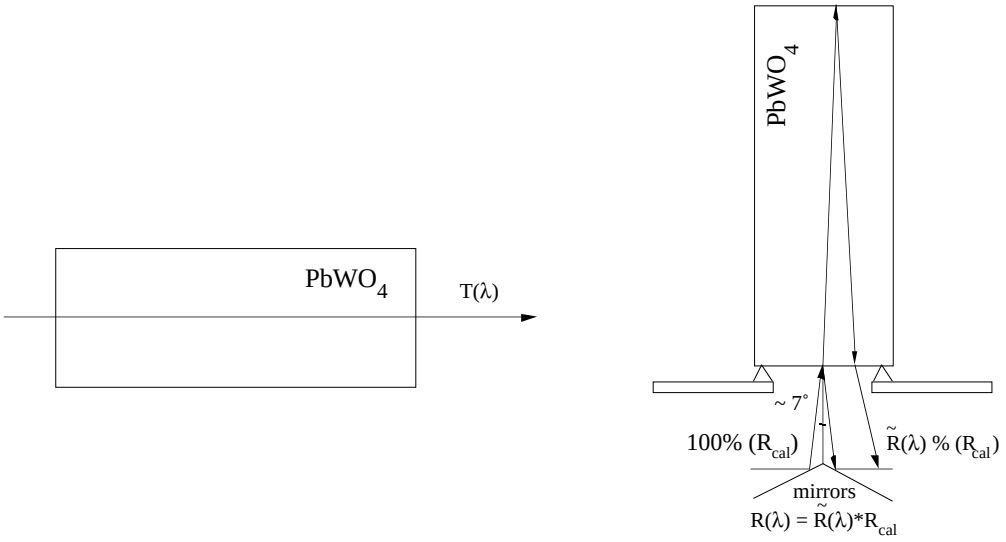

Fig. 3: Transmittance (a) and reflectance (b) measurements on a crystal.

Fig. 4 shows the two air-crystal interfaces of a sample of thickness d with the multiple reflections-transmissions of a plane wave crossing the crystal. *T* and *R* are given by the sum of infinite contributions. Even if the coherence length of the plane wave is large enough, the roughness of the air-crystal interfaces makes the contributions optically not coherent, thus *T* and *R* are given by the equations [2-4]

$$T = \frac{t^2 e^{-\alpha d}}{1 + r^2 e^{-2\alpha d}} \qquad R = r + \frac{r t^2 e^{-2\alpha d}}{1 + r^2 e^{-2\alpha d}} \tag{10}$$

where the absorption coefficient α is related to *k* by equation (1). The light intensity is rapidly decreasing so that only the first contributions are important. As an example, for n ~ 2 and $k \sim 0$, the equations (10) can be approximated to

$$\begin{aligned} T &\cong t^2 e^{-\alpha d} + t^2 r^2 e^{-3\alpha d} \\ R &\cong r + t^2 r e^{-2\alpha d} \end{aligned} \tag{11}$$

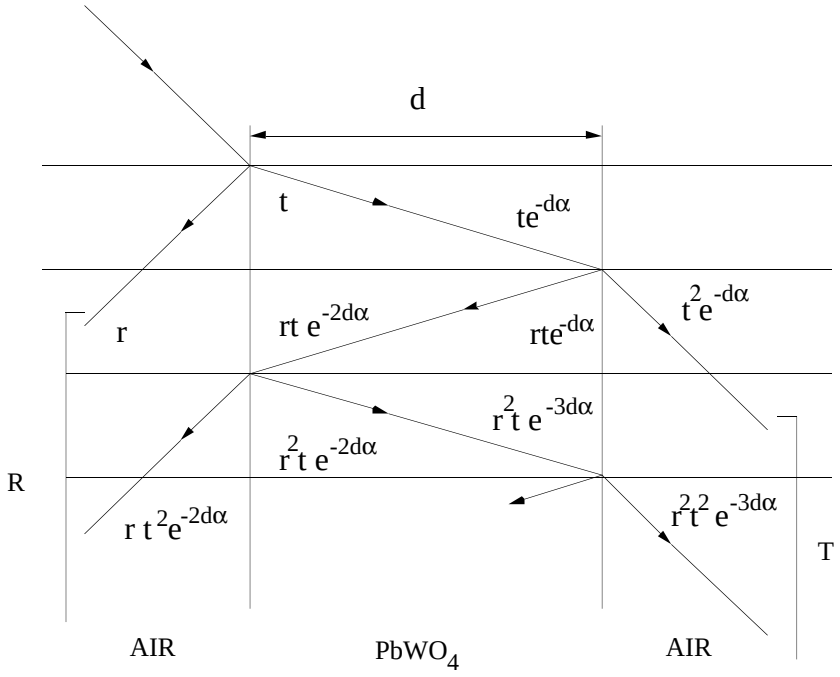

Fig. 4: Some contributions of transmittance and reflectance at quasi normal incidence of air-crystal-air interfaces.

The measurements of T and R suffer from some problems. When the opposite surfaces are not parallel, the transmitted beam is deviated respect to the direction of the beam in the reference measurement (without sample), and hits the detector in a different point (Fig. 5a). The sensitivity of the detector may be not uniform or the detector surface may not be large enough to catch entirely the spot of the beam. The imperfect parallelism of the opposite surfaces also affects the reflectance measurement. Fig. 5b shows the first contributions to the reflectance of the first and second surfaces of a thin sample without parallel surfaces. The incidence angles on the first and second surface are different and the beams reflected from the two surfaces do not have the same direction. The reflectance set-up is optically aligned by maximising the signal due to the first surface reference mirror, so that the beam reflected from the second surface hits the detector in a different point respect to the optimised condition. Therefore the imperfect parallelism of the opposite surfaces causes an error on the T and R values. This error generally depends on the crystal orientation and can seriously compromise the information deduced from $T_{//}, T_{\perp}, R_{//}$ and $R_{\perp}$. To avoid this problem it is advisable i) to evaluate the maximum beam deviation which does not affect the measured value by the spectrophotometer (generally it is of the order of few mrad) and ii) to measure the deviation angle due to the sample with a laser beam before the optical measurement. If the deviation is too large, a correction due to the effect of parallelism of the interfaces must be applied.

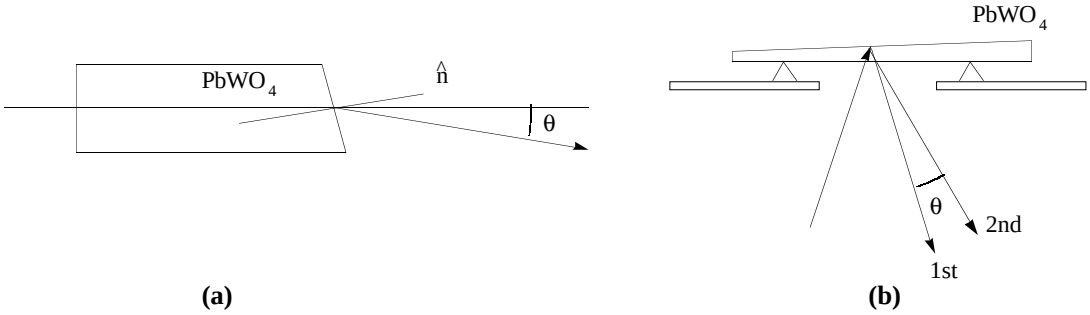

Fig. 5: Effects of non parallelism of the opposite surface on the transmittance (a) and reflectance (b) measurements.

Moreover the contributions to $T_{//}$ and $R_{//}$ are displaced respect to the contributions to $T_{\perp}$ and $R_{\perp}$. As a matter of fact, the wave corresponding to $E_{//}$ is the extraordinary ray making a γ angle with the ordinary one. Such a displacement can cause a large error on $T_{//}$ and $R_{//}$ even if the two air-crystal interfaces are perfectly parallel.

Concerning only *R*, the distance between the two main contributions, reported in equations (11) and shown in Fig. 4, depends linearly on the crystal thickness d. The first contribution hits the detector in the center while the second one in the lateral position. For long crystals (d ~20 cm) the second contribution does not reach the detector so that $R = r$. For smaller length the second contribution is detected with an efficiency $0 < \eta \leq 1$. The efficiency was evaluated by positioning the reference mirror at the distance d' from the position of the first surface of the sample on the reflectance set-up. As shown in Fig. 6, d' is the distance between the first surface and the intersection point of the prolongation of the incidence ray and of the emerging one. If the beam is entirely detected, the signal is equal to 1, otherwise is lower and the value represents the efficiency η. The reflectance *R* of the crystal is then represented by the equation

$$R = r + \eta r t^2 e^{-2\alpha d} \tag{12}$$

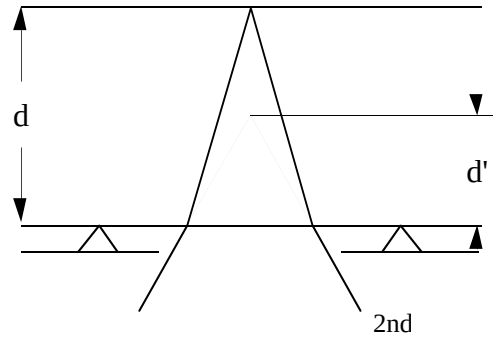

Fig. 6: The 2nd contribution of R reflected by an equivalent plane placed at the distance d', where the prolongation of the incidence ray intersects the 2nd surface contribution one.

3 - Experimental method

We measured R and T by a Lambda 9 and a 340 Perkin Elmer double beam spectrophotometers respectively, where a polariser was placed on the beam, before the sample. The linear polariser transmits in the 320-2300 nm range. A special compartment allows to measure crystals longer than the dimension of the standard cell (Fig. 7). The scheme of the device used to measure the reflection at quasi normal incidence is shown in Fig. 3b. In both devices the beam is deviated by mirrors and its *s* polarisation intensity is greater than the *p* polarisation. To optimise the signal to noise ratio , the measurement is always performed with the beam totally *s*-polarised. The crystal is oriented so that **E** is orthogonal or parallel to the Γ plane.

The instrument reference value was measured without sample for the transmittance and for the reflectance measurement with a first surface reference mirror (NBS SRM 2003) whose reflectance in the 200-3500 nm range is known.

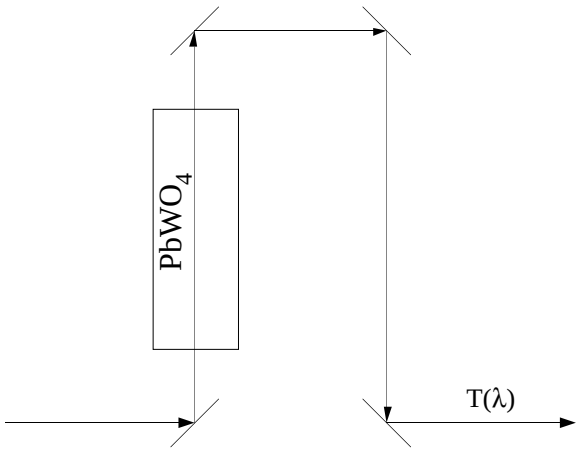

Fig. 7: Set-up for transmittance measurements on long crystal.

4 - Results and discussion

In the case of PWO-522, the sample dimensions are 2x2x1 cm. Only the two 2x2 cm^2 faces are polished and are used for the optical measurements. The 1 cm length of the sample does not allow to distinguish the extraordinary from the ordinary ray and no information about the Γ plane is available. Fig. 8 shows *T* and *R* measured with unpolarised light in the range 330-850 nm. These measurements are not affected by the errors previously discussed in section 2.2 and the second surface contribution was entirely detected. Assuming the crystal to be isotropic, we searched for the (n (λ), α (λ))

solutions of equations (11) by a numerical method. The results are reported in Fig. 9 and 10. The absorption coefficient α increases strongly near 350 nm.

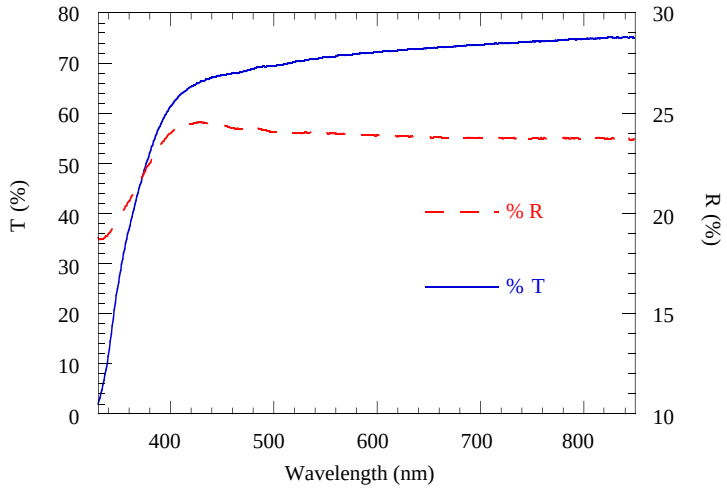

Fig. 8: T and R with unpolarised light; PWO-522 sample.

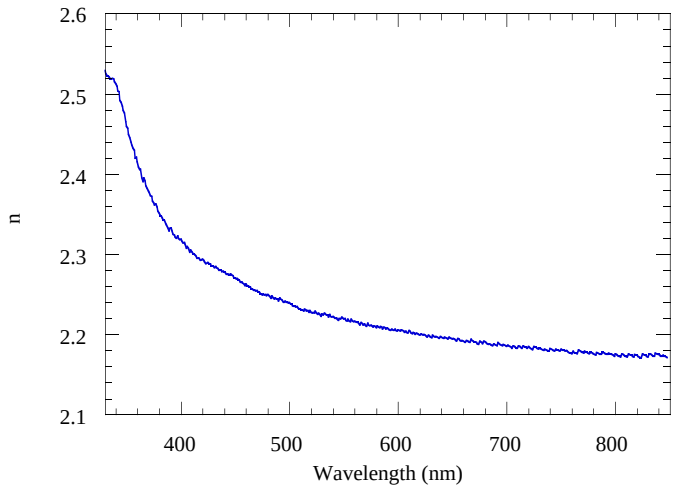

Fig. 9: n versus wavelength for PWO-522 sample.

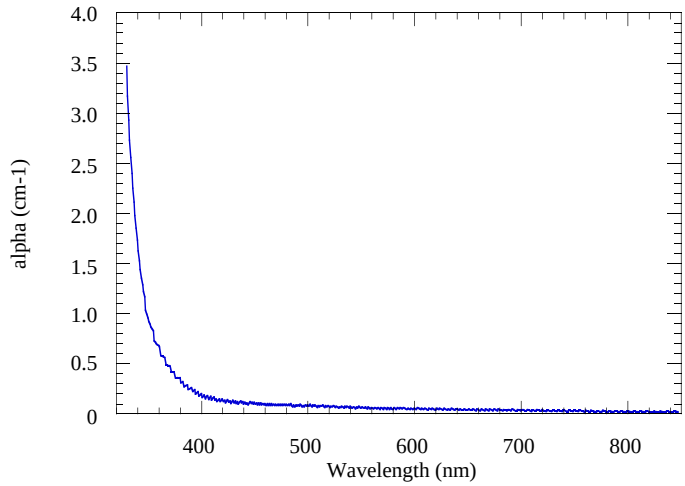

Fig. 10: α versus wavelength for PWO-522 sample.

In the case of PWO-N30, the sample dimensions are 2x2x23 cm^3 and all the faces are polished. Fig. 11 shows the splitting of a laser beam impinging orthogonally on the 2x2 cm^2 surface (Σ) closest to the N30 mark. The second column of Table 1 lists the γ angle at the wavelength of Ar and HeNe lasers. The largest angle is measured at the shorter wavelength. The Γ plane is almost orthogonal with the N30 marked 2x23 cm^2 surface. More precisely in the direction of the wave propagation, the Γ plane makes the δ angle with the N30 marked surface equal to 100° ± 1°. The $R_{//}$ and $R_{\perp}$ measured on the Σ surface, are reported in Fig. 12. In the examined wavelength range, $R_{//}$ is always lower than $R_{\perp}$, therefore n_{ext} is lower then n_{ord}. The crystal length is such that the 2nd surface contribution on R is not detected, then $R_{//} = r_{//}$ and $R_{\perp} = r_{\perp}$. The $n_{ord}(\lambda)$ and $n_{mix}(\lambda)$ are calculated from $r_{\perp}$ and $r_{//}$ considering $k = 0$ and they are shown in Fig. 13. Their values at the Ar and HeNe laser wavelengths are listed in the 3rd and 4th columns of Table 1.

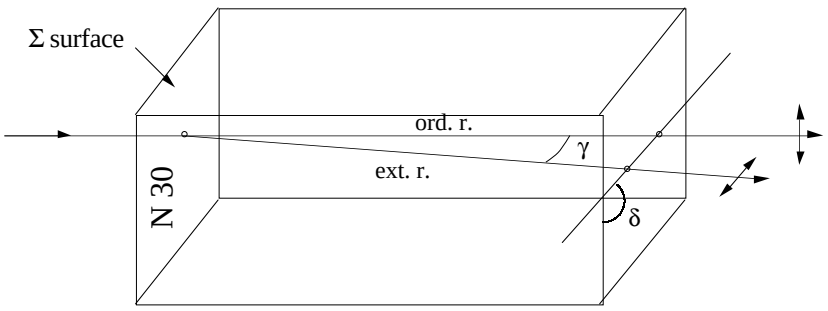

Fig. 11: Splitting of a laser beam impinging orthogonally on the (2x2) cm surface (Σ) closest to the N30 mark. In the direction of the wave propagation, the Γ plane makes the δ = 100° ± 1° angle with the N30 marked surface.

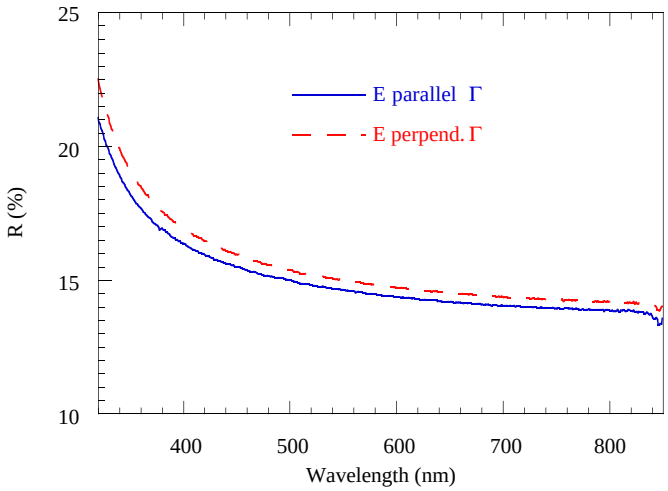

Fig. 12: $R_{//}$ and $R_{\perp}$ measured on the Σ surface of PWO-N30. $R_{//} = r_{//}$ and $R_{\perp} = r_{\perp}$. The 2nd surface contribution on R was not caught by the detector.

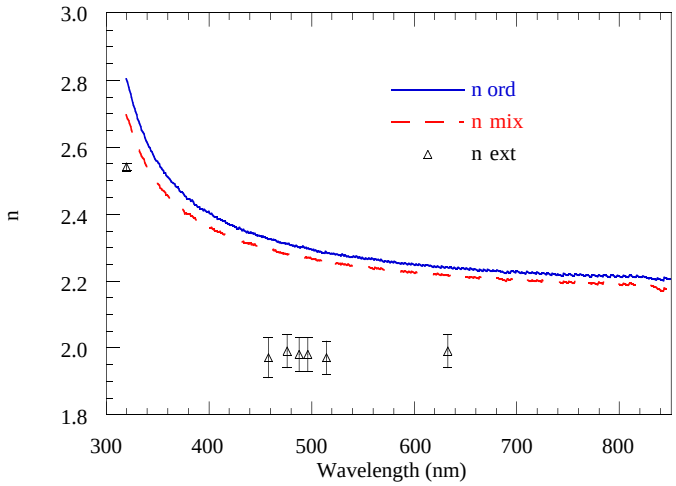

Fig. 13: $n_{ord}(\lambda)$, $n_{mix}(\lambda)$ and n_{ext} at the Ar and HeNe laser wavelengths for PWO-N30 sample.

Table 1

Crystal PWO-N30

λ (nm)	γ (deg)	n ord	n mix	n ext
457.9	2.61 ± 0.07	2.32 ± 0.01	2.30 ± 0.01	1.97 ± 0.06
476.5	2.37 ± 0.07	2.31 ± 0.01	2.28 ± 0.01	1.99 ± 0.05
488.0	2.37 ± 0.07	2.30 ± 0.01	2.27 ± 0.01	1.98 ± 0.05
496.5	2.37 ± 0.07	2.30 ± 0.01	2.27 ± 0.01	1.98 ± 0.05
514.5	2.37 ± 0.07	2.29 ± 0.01	2.26 ± 0.01	1.97 ± 0.05
632.8	1.93 ± 0.07	2.24 ± 0.01	2.22 ± 0.01	1.99 ± 0.05

The β angle and n_{ext} can be determined from the knowledge of γ, n_{ord} and n_{mix}. The β angle does not depend on λ and it is related to the orientation of the crystallographic axis. In order to minimise the propagation of the experimental error on β value, we transform equation (8) into

$$\frac{n_{ext}}{n_{ord}} = \tan\beta / \tan(\beta + \gamma) \tag{13}$$

Using equation (13), equation (2) becomes

$$\frac{n_{mix}}{n_{ord}} = \sin\beta \sqrt{1 + \frac{1}{\tan^2(\beta+\gamma)}} \tag{14}$$

The β angle is then obtained by minimising the merit function (MF) defined as

$$MF = \sqrt{Max\left\{ \frac{\left(\frac{n_{mix}}{n_{ord}}(\lambda_i) - \sin\beta\sqrt{1+[\tan(\beta+\gamma(\lambda_i))]^{-2}} \right)^2}{Err^2\left(\frac{n_{mix}}{n_{ord}}(\lambda_i)\right)} \right\}} \qquad i = 1,2,\ldots 6 \tag{15}$$

where $\lambda_1,\lambda_2,\ldots\lambda_6$ are the Ar and HeNe laser wavelengths, $Err\left(\frac{n_{mix}}{n_{ord}}(\lambda_i)\right) \cong 0.003$ and the error due to γ is negligible with respect to $Err\left(\frac{n_{mix}}{n_{ord}}(\lambda_i)\right)$.

The error $Err\left(\frac{n_{mix}}{n_{ord}}(\lambda_i)\right)$ is related only to the spectrophotometer sensitivity. As a matter of fact

i) the error of the absolute value of the reference mirror affects in the same way n_{ord} and n_{mix} without changing the ratio n_{mix}/n_{ord};
ii) the error due to the fluctuation of the baseline can be neglected because the $R_{//}$ and $R_{\perp}$ measurements were consecutive.

The merit function computed with the values reported in Table 1 is less than 1 for β = 72° ± 2° (Fig. 14). The extraordinary refractive index is then calculated by equation (13) and the values are reported in the 5th column of Table 1 and in Fig. 13. At the wavelengths where γ is not known, n_{ext} could be computed by equation (2) but the error is very large for a β angle close to 90°. A better evaluation of n_{ext} can be obtained from the measurement of R on a large surface 2x23 cm^2 with **E** almost parallel to the optical axis. Unfortunately the compartment of Lambda 9 spectrophotometer does not allow the

position of the sample in this way. We tried to rotate the light polarisation, instead of the sample, but the spectral measurement was noisy because of the weak signal. We kept only the measurement at 320 nm, where the crystal is not transparent, and we obtained $n_{ext} = 2.54 \pm 0.01$. At the same wavelength $n_{ord} = 2.80 \pm 0.01$, so that $n_{ord}-n_{ext} \sim 0.26$. Taking into account the results reported in Table 1, the difference $n_{ord}-n_{ext}$ seems to be about a constant in the considered wavelength range. The PWO-522 refractive index is included between n_{ord} and n_{ext}.

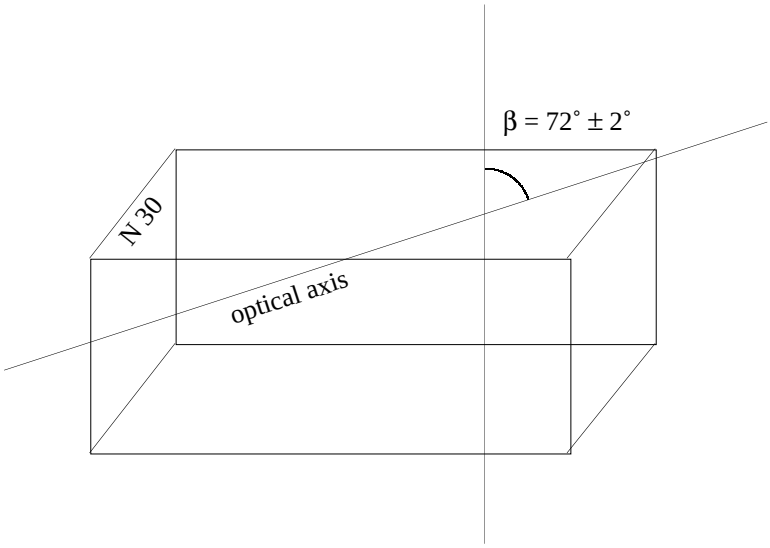

Fig. 14: Orientation of the crystal optical axis.

To obtain information on the imaginary part of refractive index, the transmittance measurement is necessary. By our instrument it was possible to measure only $T_{\perp}$ because $T_{//}$ was seriously affected by the displacement of extraordinary ray as described at the end of section 2.2. Fig. 15 shows $T_{\perp}$ and the absorption coefficient α related to the imaginary part (k) of the ordinary refractive index. The absorption coefficient was computed from $T_{\perp}$ by eq. (11) using the previously determined n_{ord} and it is lower than the one of PWO-522. As an example α_{N30} (λ = 500 nm) = $(2.8 \pm 0.2)\ 10^{-2}\ cm^{-1}$ and α_{522} (λ = 500 nm) = $(6.8 \pm 0.4)\ 10^{-2} cm^{-1}$.

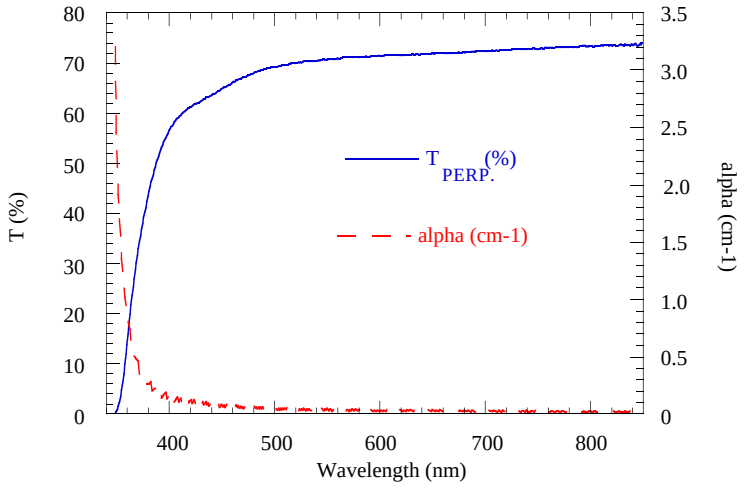

Fig. 15: $T_{\perp}$ and the absorption coefficient α_{ord} versus wavelengths for PWO-N30 sample.

In the case of PWO-1024, the sample dimensions are 2x2x21.5 cm^3 and all faces are polished. The Γ plane makes $\delta = 57° \pm 1°$ with the 2x21.5 cm^2 marked surface. Fig. 16 shows the $R_{//}$ and $R_{\perp}$ measured on Σ surface and Fig. 17 shows the computed n_{ord} and n_{mix}. Table 2 lists the γ angle values measured at various laser wavelengths, n_{ord} and n_{mix} calculated by $R_{\perp}$ and $R_{//}$, and n_{ext} calculated by eq. (13), for $\beta = 76° \pm 2°$ corresponding to MF ≤ 1.

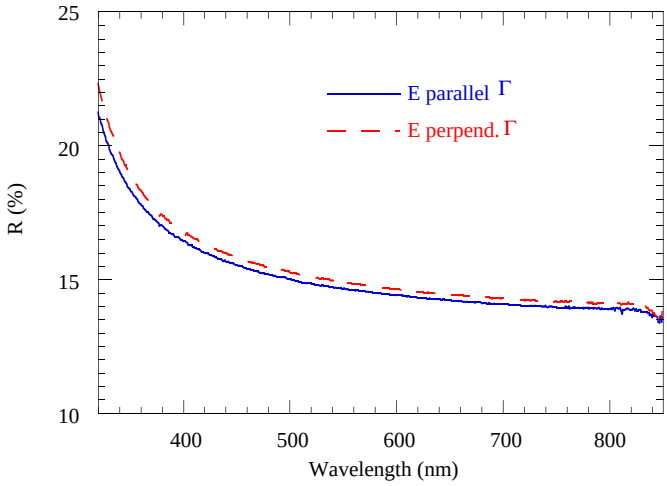

Fig. 16: $R_{//}$ and $R_{\perp}$ versus wavelengths for PWO-1024 sample.

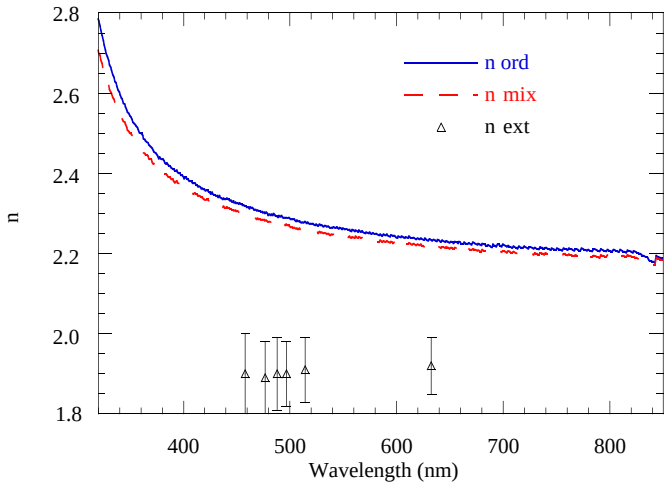

Fig. 17: $n_{ord}(\lambda)$, $n_{mix}(\lambda)$ and n_{ext} at the Ar and HeNe laser wavelengths for PWO-1024 sample.

Table 2
Crystal PWO-1024

λ (nm)	γ (deg)	n_{ord}	n_{mix}	n_{ext}
457.9	2.53 ± 0.07	2.32 ± 0.01	2.30 ± 0.01	1.9 ± 0.1
476.5	2.33 ± 0.07	2.30 ± 0.01	2.28 ± 0.01	1.89 ± 0.09
488.0	2.26 ± 0.07	2.29 ± 0.01	2.27 ± 0.01	1.90 ± 0.09
496.5	2.20 ± 0.07	2.29 ± 0.01	2.27 ± 0.01	1.90 ± 0.08
514.5	2.13 ± 0.07	2.28 ± 0.01	2.26 ± 0.01	1.91 ± 0.08
632.8	1.86 ± 0.07	2.23 ± 0.01	2.22 ± 0.01	1.92 ± 0.07

Both n_{ord} and n_{ext} are equal inside the experimental error to those of PWO-N30, and we can conclude that the Nb^{5+} doping affects the real part of the crystal refractive index by less than 0.01 (the experimental error).

5 - Conclusions

For long crystals (with length of about 20 cm) the optical axis orientation and the ordinary and extraordinary refractive index were determined by means of the propagation of laser beams and by reflectance and transmittance measurements with polarised light at almost normal incidence. The $PbWO_4$ extraordinary refractive index is lower than the ordinary one and both seem not to be affected by a 30 ppm Nb^{5+} doping. For both long

crystals the position of the identification mark, placed on a side of a long surface, and the optical axis are oriented in the same way(see Fig. 14). Moreover the angles between the growth axis and the optical axis are very similar and they are in good agreement with the value reported in [5].

The $T_{//}$ measurements was seriously affected by the displacement of the extraordinary ray. Work is in progress to determine the imaginary part of the extraordinary refractive index.

6 - References

[1] M. Born, and E. Wolf, *Principles of Optics*, 3th edition, Pergamon Press, Oxford (1965).

[2] O. S. Heavens, *Optical Properties of Thin Solid Films*, Dover, New York (1965).

[3] H. Walter, Z. Physik, 105, 269 (1937).

[4] H. E. Bennett, and J. H. Bennett, *Physics of Thin Films*, G. Hass and R. E. Thun Eds., Academic, New York (1967).

[5] P. Lecoq, I. Dafinei, E. Auffray, M. Schneegans, M.V. Korzhik, V.B. Pavlenko, A. A. Fedorov, A.N. Annenkov, V. L. Kostylev, V. D. Ligun, CERN-PPE/ 94-225, CMS-TN/ 94-308 (1994).